Physics Letters A 459 (2023) 128611

Contents lists available at ScienceDirect

Physics Letters A

journal homepage: www.elsevier.com/locate/pla

Transparent boundary conditions for the nonlocal nonlinear Schrödinger equation: A model for reflectionless propagation of PT-symmetric solitons

M.E. Akramov [a], J.R. Yusupov [b,*], M. Ehrhardt [c], H. Susanto [d], D.U. Matrasulov [e]

[a] National University of Uzbekistan, Universitet Str. 4, 100174, Tashkent, Uzbekistan
[b] Kimyo International University in Tashkent, Usman Nasyr Str. 156, 100121, Tashkent, Uzbekistan
[c] Bergische Universitat Wuppertal, Gaußstrasse 20, D-42119, Wuppertal, Germany
[d] Khalifa University, 127788, Abu Dhabi, United Arab Emirates
[e] Turin Polytechnic University in Tashkent, Niyazov Str. 17, 100095, Tashkent, Uzbekistan

ARTICLE INFO

Article history:
Received 17 October 2022
Received in revised form 22 December 2022
Accepted 23 December 2022
Available online 2 January 2023
Communicated by B. Malomed

Keywords:
Transparent boundary conditions
Nonlocal nonlinear Schrödinger equation
PT-symmetric solitons

ABSTRACT

We consider the problem of reflectionless propagation of PT-symmetric solitons described by the nonlocal nonlinear Schrödinger equation on a line in the framework of the concept of transparent boundary conditions for evolution equations. Transparent boundary conditions for the nonlocal nonlinear Schrödinger equation are derived. The absence of backscattering at the artificial boundaries is confirmed by the numerical implementation of the transparent boundary conditions.

1. Introduction

Modeling of wave dynamics in various media is of practical importance in the fields of optics, optoelectronics, fluid dynamics, acoustics and communication technology. An important problem to be solved by such models is tunable wave propagation, which means achieving ballistic and diffusive states or absence of backscattering and reflection in a certain subdomains. In quantum mechanics, such a goal can be achieved by constructing a suitable scattering matrix that ensures the absence of reflection.

However, in the case of nonlinear wave propagation, one cannot use a scattering matrix and must develop efficient mathematical tools to describe reflectionless propagation. One of these tools can be based on the use of the concept of so-called *"transparent boundary conditions (TBCs)"* (other names are "artificial boundary conditions" and "absorbing boundary conditions"). The concept was previously applied to the linear [1] and nonlinear [2–5] Schrödinger equations. Recently, the application of the TBC concept to Dirac [6] and Klein-Gordon equations [7,8], including the nonlinear Klein-Gordon equation [8–11] was shown. Extensions of TBCs for evolution equations on graphs can be found in references [12,13].

The basic idea of the TBC concept can be formulated as follows: For a given partial differential equation formulated as an initial value problem in a finite domain, it is required that the solution in one domain should match that in the entire space restricted to the finite domain. This can be achieved by artificial boundary conditions, which have a rather complicated form (e.g., for Schrödinger or Dirac equations given in terms of fractional derivatives are [1,6]).

In this paper we extend the TBC concept for the *nonlocal nonlinear Schrödinger equation (NNLS)* describing the dynamics of PT-symmetric solitons. The NNLS equation was first introduced by Ablowitz and Musslimani [14], who showed the integrability of the problem and obtained their soliton solutions. Later it was used in various contexts in Refs. [14–28]. The NNLS equation describes the dynamics of solitons in media with self-induced PT-symmetric nonlinearity (such nonlinearity may be present, for example, in an optical waveguide with self-induced gain loss). Our proposed model accounts for reflectionless propagation of solitons in such media. The transparent boundary conditions derived here provide mathematical constraints that ensure that there is no backscattering. In practical applications of boundary conditions, e.g., for branched waveguides, they can provide physically acceptable constraints on the equivalence of the usual weight continuity and Kirchhoff's rules with the transparent boundary conditions at the branching point (see, e.g., Ref. [12] for details). We note that reflectionless

* Corresponding author.
E-mail address: j.yusupov@kiut.uz (J.R. Yusupov).

https://doi.org/10.1016/j.physleta.2022.128611
0375-9601/

wave motion in nonlinear systems was considered earlier in different contexts (see, e.g., Ref. [29]).

The motivation for studying reflectionless soliton propagation in low-dimensional systems arises from the importance of practical applications of such a problem in various structures encountered in optics, condensed matter and fluid dynamics. In particular, the model developed in this work can be used to describe soliton generation and propagation in optical fiber networks where each branch has a self-induced gain-loss and other branched waveguides generate a self-induced PT-symmetric potential. Furthermore, the experimental implementation of such a model is of importance for the development and practical implementation of various PT-symmetric optical fiber networks capable of generating solitonic pulses and tunable signal propagation. With an effective tool for reflectionless soliton propagation, signal loss, backscattering and modulation can be controlled by tuning the signal generation.

This paper is organized as follows. In the next section, we briefly recall soliton solutions and conserving quantities for the NNLS equation on a line. In Section 3, we derive the transparent boundary conditions for the NNLS equation. In Section 4, we demonstrate our numerical implementation of such boundary conditions and show the results of numerical experiments in Section 5. Finally, Section 6 contains the concluding remarks.

2. Soliton solutions of the nonlocal nonlinear Schrödinger equation

Here we briefly recall basic results on the NNLS equation on a line, following Ref. [14]. The nonlocal nonlinear Schrödinger equation is given as [14]

$$\mathrm{i}\partial_t q(x,t) + \partial_x^2 q(x,t) + 2q(x,t)q^*(-x,t)q(x,t) = 0, \tag{1}$$

where q^* denotes the complex conjugate of q and the potential, which can be defined as $V(x,t) = 2\,q(x,t)\,q^*(-x,t)$, has the PT symmetric property, i.e. $V(x,t) = V^*(-x,t)$. We note that the nonlocality of Eq. (1) results from the fact that the evolution of the field $q(x,t)$ at coordinate x always requires information from the opposite point $-x$. For the above NNLS equation, there are many different types of soliton solutions, namely breathing, periodic, rational, and others. A single soliton solution can be found by the inverse scattering method as given in Ref. [14]:

$$q(x,t) = -\frac{2(\eta_1+\bar\eta_1)\,e^{\mathrm{i}\bar\theta_1}\,e^{4\mathrm{i}\bar\eta_1^2 t}\,e^{-2\bar\eta_1 x}}{1+e^{\mathrm{i}(\theta_1+\bar\theta_1)}\,e^{-4\mathrm{i}(\eta_1^2-\bar\eta_1^2)t}\,e^{-2(\eta_1+\bar\eta_1)x}}, \tag{2}$$

with η_1, $\bar\eta_1$, θ_1, and $\bar\theta_1$ being real constants. The traveling soliton solution of Eq. (1) can be written as [15]

$$q(x,t) = \frac{\alpha_1\,e^{-\Delta/2}\,e^{(\bar\xi_{1R}-\xi_{1R})+i(\bar\xi_{1I}-\xi_{1I})}}{2[\cosh(\chi_1)\cos(\chi_2)+\mathrm{i}\sinh(\chi_1)\sin(\chi_2)]}, \tag{3}$$

where $\xi_{1R} = -k_{1I}(x+2k_{1R}t)$, $\xi_{1I} = k_{1R}x - (k_{1I}^2 - k_{1R}^2)t$, $\bar\xi_{1R} = -\bar k_{1I}(x-2\bar k_{1R}t)$, $\bar\xi_{1I} = \bar k_{1R}x - (\bar k_{1R}^2 - \bar k_{1I}^2)t$, $\Delta_R = \log\left(\frac{|\alpha_1|^2|\beta_1|^2}{|k_1+\bar k_1|^2}\right)$, $\Delta_I = -\frac{\mathrm{i}}{2}\log\left(\frac{\alpha_1\beta_1(k_1^*+\bar k_1^*)^2}{\alpha_1^*\beta_1^*(k_1+\bar k_1)^2}\right)$, $e^{\Delta} = -\frac{\alpha_1\beta_1}{(k_1+\bar k_1)^2}$, $\chi_1 = (\xi_{1R}+\bar\xi_{1R}+\Delta_R)/2$ and $\chi_2 = (\xi_{1I}+\bar\xi_{1I}+\Delta_I)/2$.

The integrability of the problem was proved in [14], which means that the NNLS equation has many conservation laws. In particular, two important conservation quantities, the norm and the energy, were derived in [14] and can be written as

$$N(t) = \int_{-\infty}^{+\infty} q(x,t)q^*(-x,t)\,dx,$$

$$E(t) = \int_{-\infty}^{+\infty}\left[\frac{\partial}{\partial x}q(x,t)\cdot\frac{\partial}{\partial x}q^*(-x,t) + q^2(x,t)\cdot q^{*2}(-x,t)\right]dx. \tag{4}$$

The above soliton solutions of Eq. (1) are obtained assuming asymptotic boundary conditions at infinity, i.e. $q(x,t)\to 0$ at $x\to\pm\infty$. In the next section, we impose additional (artificial) boundary conditions for a given finite interval $[-L,L]$ that allow an almost reflection-free transmission of a soliton through the points $\pm L$.

3. Transparent boundary conditions for the nonlocal nonlinear Schrödinger equation

Here we consider the problem of transparent boundary conditions for the NNLS equation (1). To derive TBCs for the nonlocal nonlinear Schrödinger equation, we use the so-called *potential approach*, which was proposed earlier in [2] and used to derive TBCs for coupled nonlinear Schrödinger equations [30]. Within the framework of this approach, the NNLS equation can be formally reduced to the linear Schrödinger equation

$$\mathrm{i}\partial_t q(x,t) + \partial_x^2 q(x,t) + V(x,t)q(x,t) = 0, \tag{5}$$

with the potential is $V(x,t) = 2q(x,t)q^*(-x,t)$. In the remainder of this section, we invoke the same procedure and derive TBCs at the end.

To do so, we introduce a new unknown $Q(x,t)$, which is given by the relation

$$Q(x,t) = e^{-\mathrm{i}\mathcal{V}(x,t)}\,q(x,t), \tag{6}$$

where

$$\mathcal{V}(x,t) = \int_0^t V(x,s)\,ds. \tag{7}$$

The temporal and spatial derivatives of q can be written as derivatives of Q as

$$\partial_t q = e^{\mathrm{i}\mathcal{V}}(\partial_t + \mathrm{i}V)\,Q, \tag{8}$$

and

$$\partial_x^2 q = \mathrm{i}e^{\mathrm{i}\mathcal{V}}(\partial_x^2 Q + 2\mathrm{i}\partial_x\mathcal{V}\partial_x Q + \mathrm{i}Q\,\partial_x^2\mathcal{V} - (\partial_x\mathcal{V})^2 Q). \tag{9}$$

As a result, we obtain the Schrödinger equation in terms of $Q(x,t)$ as

$$L(x,t,\partial_x,\partial_t)Q = \mathrm{i}\partial_t Q + \partial_x^2 Q + A\partial_x Q + BQ = 0, \tag{10}$$

where $A = 2\mathrm{i}\partial_x\mathcal{V}$ and $B = (\mathrm{i}\partial_x^2\mathcal{V} - (\partial_x\mathcal{V})^2)$. Using the pseudo-differential operator calculus one can linearize Eq. (10) as

$$\begin{aligned} L &= (\partial_x + \mathrm{i}\Lambda^-)(\partial_x + \mathrm{i}\Lambda^+) \\ &= \partial_x^2 + \mathrm{i}(\Lambda^+ + \Lambda_-)\partial_x + \mathrm{i}\,\mathrm{Op}(\partial_x\lambda^+) - \Lambda^+\Lambda^-, \end{aligned} \tag{11}$$

where λ^+ is the principal symbol of the operator Λ^+ and $\mathrm{Op}(p)$ denotes the associated operator of a symbol p. The Eqs. (10) and (11) lead to the system of operators

$$\begin{aligned} &i(\Lambda^+ + \Lambda^-) = A \\ &i\,\mathrm{Op}(\partial_x\lambda^+) - \Lambda^+\Lambda^- = i\partial_t + B. \end{aligned} \tag{12}$$

Since two functions A and B correspond to zero-order operators ($\mathrm{Op}(a) = A$ and $\mathrm{Op}(b) = B$), one obtains the symbolic system of equations as

$$\mathrm{i}(\lambda^+ + \lambda^-) = a$$
$$\mathrm{i}\partial_x\lambda^+ - \sum_{\alpha=0}^{+\infty}\frac{(-1)^\alpha}{\alpha!}\partial_\tau^\alpha\lambda^-\partial_t^\alpha\lambda^+ = -\tau + b. \tag{13}$$

An asymptotic evolution in the inhomogeneous symbols can be written as

$$\lambda^\pm \sim \sum_{j=0}^{+\infty}\lambda^\pm_{1/2-j/2}. \tag{14}$$

One can determine the 1/2-order terms in the first relation of the system (13) by substituting the expansion (14) into Eq. (13):

$$\lambda^-_{1/2} = -\lambda^+_{1/2}, \quad \lambda^+_{1/2} = \pm\sqrt{-\tau}. \tag{15}$$

Here the choice $\lambda^+_{1/2} = \pm\sqrt{-\tau}$ corresponds to the Dirichlet-to-Neumann operator. The system of equations for the zeroth-order terms can be written as

$$\lambda^-_0 = -\lambda^+_0 - \mathrm{i}a,$$
$$\mathrm{i}\partial_x\lambda^+_{1/2} - (\lambda^-_0\lambda^+_{1/2} + \lambda^+_0\lambda^-_{1/2}) = 0. \tag{16}$$

Then, from Eq. (16) we obtain

$$\lambda^+_0 = -\mathrm{i}\frac{a}{2} = \frac{1}{2}\partial_x\mathcal{V},$$
$$\lambda^-_0 = -\lambda^+_0 - \mathrm{i}a = \frac{1}{2}\partial_x\mathcal{V}. \tag{17}$$

Since $\partial_t^\alpha\lambda^\pm_{-1/2} = \partial_\tau^\alpha\lambda^\pm_0 = 0$, $\alpha \in N$, for the terms of order $-1/2$ we get

$$\mathrm{i}(\lambda^+_{-1/2} + \lambda^-_{-1/2}) = 0,$$
$$\mathrm{i}\partial_x\lambda^+_0 - (\lambda^-_{-1/2}\lambda^+_{1/2} + \lambda^+_0\lambda^-_0 + \lambda^+_{-1/2}\lambda^-_{1/2}) = b. \tag{18}$$

From Eq. (18) we obtain

$$\lambda^\pm_{-1/2} = 0. \tag{19}$$

In the same way one can obtain the terms of the next order as

$$\lambda^-_{-1} = -\lambda^+_{-1}, \quad \lambda^+_{-1} = \mathrm{i}\frac{\partial_x V}{4\tau}. \tag{20}$$

As a result the first-order approximation reads

$$\partial_x q|_{x=-L} - e^{-\mathrm{i}\frac{\pi}{4}}e^{\mathrm{i}\mathcal{V}}\partial_t^{1/2}(e^{-\mathrm{i}\mathcal{V}}q)\big|_{x=-L} = 0, \tag{21a}$$
$$\partial_x q|_{x=L} + e^{-\mathrm{i}\frac{\pi}{4}}e^{\mathrm{i}\mathcal{V}}\partial_t^{1/2}(e^{-\mathrm{i}\mathcal{V}}q)\big|_{x=L} = 0. \tag{21b}$$

The second-order approximation is

$$\partial_x q|_{x=-L} - e^{-\mathrm{i}\frac{\pi}{4}}e^{\mathrm{i}\mathcal{V}}\partial_t^{1/2}(e^{-\mathrm{i}\mathcal{V}}q)\big|_{x=-L} - \mathrm{i}\frac{\partial_x V}{4}e^{\mathrm{i}\mathcal{V}}I_t(e^{-\mathrm{i}\mathcal{V}}q)\big|_{x=-L} = 0, \tag{22a}$$
$$\partial_x q|_{x=L} + e^{-\mathrm{i}\frac{\pi}{4}}e^{\mathrm{i}\mathcal{V}}\partial_t^{1/2}(e^{-\mathrm{i}\mathcal{V}}q)\big|_{x=L} + \mathrm{i}\frac{\partial_x V}{4}e^{\mathrm{i}\mathcal{V}}I_t(e^{-\mathrm{i}\mathcal{V}}q)\big|_{x=L} = 0. \tag{22b}$$

The operator $\partial_t^{1/2}$, which denotes the half order fractional time derivative operator, is defined as

$$\partial_t^{1/2}f(t) = \frac{1}{\sqrt{\pi}}\partial_t\int_0^t\frac{f(s)}{\sqrt{t-s}}\,ds,$$

and the operator $I_t(f)$ is

$$I_t f(t) = \int_0^t f(s)\,ds.$$

4. A discretization scheme for the transparent boundary conditions

In this section, we present a numerical scheme for Eq. (1) and the numerical implementation of the transparent boundary conditions (21) and (22). We have chosen the finite difference scheme of Duran–Sánz-Serna [31], a second order scheme based on the implicit midpoint rule

$$\mathrm{i}\frac{q_j^n - q_j^{n-1}}{\Delta t} + D_x^2\frac{q_j^n + q_j^{n-1}}{2} + 2\Big(\frac{q_j^n + q_j^{n-1}}{2}\Big)^2\frac{\overline{q^n_{J-j}} + \overline{q^{n-1}_{J-j}}}{2} = 0, \tag{23}$$

with the standard second-order difference quotient

$$D_x^2 q_j^n = \frac{1}{\Delta x^2}(q^n_{j-1} - 2q^n_j + q^n_{j+1}), \tag{24}$$

with Δx and Δt being the space and time discretization steps. Here $\overline{q_j^n}$ denotes the complex conjugate of q_j^n, J is the number of discretized spatial steps, and q_j^n denotes the approximate value of q at spatial coordinate x_j and time t_n.

We now give an effective discretization scheme for the TBC, which is implemented together with (23). We give the scheme only for $x = L$, saying that the implementation for the left-hand side (at $x = -L$) can be done in the same way. We approximate the fractional differential operator using the numerical quadrature formula given in [2]

$$\partial_t^{1/2}f(t_n) \approx \sqrt{\frac{2}{\Delta t}}\sum_{k=0}^n\beta_k f^{n-k}. \tag{25}$$

Here the terms of the sequence $\{f_n\}_{n\in N}$ are complex numbers, which approximate $\{f(t_n)\}_{n\in N}$ and the sequence $(\beta_k)_{k\in N}$ is defined by

$$(\beta_0, \beta_1, \beta_2, \beta_3, \beta_4, \beta_5, \dots) = \Big(1, -1, \frac{1}{2}, -\frac{1}{2}, \frac{1\cdot 3}{2\cdot 4}, -\frac{1\cdot 3}{2\cdot 4}, \dots\Big). \tag{26}$$

The function $\mathcal{V}(x,t)$ defined in (7) can be approximated by the trapezoidal rule as

$$\mathcal{V}_j^n = \Delta t\Big[\sum_{k=1}^{n-1}V_j^k + \frac{1}{2}(V_j^0 + V_j^n)\Big] \quad \text{for } n \geq 2, \tag{27}$$

with $\mathcal{V}_j^0 = 0$ and $\mathcal{V}_j^1 = \frac{1}{2}(V_j^0 + V_j^1)$, where V_j^n is defined as

$$V_j^n = 2q_j^n\overline{q^n_{J-j}}. \tag{28}$$

Next, the term $e^{\mathrm{i}\mathcal{V}}$ is written as

$$P_j^n := \exp(\mathrm{i}\mathcal{V}_j^n) = \exp\left\{\mathrm{i}\Delta t\left[\sum_{k=1}^{n-1}V_j^k + \frac{1}{2}(V_j^0 + V_j^n)\right]\right\}. \tag{29}$$

One can rewrite Eq. (29) as a recurrence formula

$$P_j^n = P_j^{n-1}\exp\Big(\frac{\mathrm{i}\Delta t}{2}(V_j^{n-1} + V_j^n)\Big). \tag{30}$$

The first order approximation for the TBC operator (21) at the left ($j = 0$) and right ($j = J$) boundaries is approximated using the discrete convolutions

$$\Lambda_1^n = e^{-\mathrm{i}\pi/4}\sqrt{\frac{2}{\Delta t}}P_j^n\sum_{k=0}^n\beta_k\frac{q_j^{n-k}}{P_j^{n-k}}. \tag{31}$$

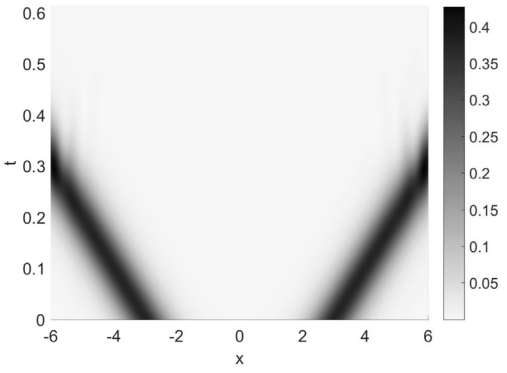

Fig. 1. Evolution of the soliton profile with TBCs imposed at both (left and right) end points.

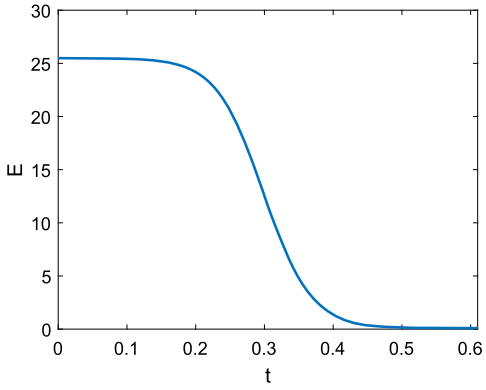

Fig. 2. The plot of the energy versus time in the finite domain $x \in [-L, L]$.

Then all the values of the solution (at the boundaries and other intermediate values) can be calculated via solving the system of nonlinear equations as

$$\frac{q_1^n - q_0^n}{\Delta x} - e^{-\mathrm{i}\pi/4}\sqrt{\frac{2}{\Delta t}}P_0^n \sum_{k=0}^{n}\left(\beta_k \frac{q_0^{n-k}}{P_0^{n-k}}\right) = 0, \tag{32a}$$

$$\frac{q_J^n - q_{J-1}^n}{\Delta x} + e^{-\mathrm{i}\pi/4}\sqrt{\frac{2}{\Delta t}}P_J^n \sum_{k=0}^{n}\left(\beta_k \frac{q_J^{n-k}}{P_J^{n-k}}\right) = 0, \tag{32b}$$

and the Eq. (23) with respect to q_j^n. Note that the values of q_j^n to be found also exist in P_j^n and here we have written Eqs. (32) in short form. Applying the same approach, one can continue to discretize the second-order approximation. Thus, the integral term can be approximated as

$$I_j^n = \Delta t\left[\sum_{k=1}^{n-1}\frac{q_j^k}{P_j^k} + \frac{1}{2}\left(\frac{q_j^0}{P_j^0} + \frac{q_j^n}{P_j^n}\right)\right]. \tag{33}$$

In the same way we construct a recurrence formula for I_j^n

$$I_j^n = I_j^{n-1} + \frac{\Delta t}{2}\left(\frac{q_j^{n-1}}{P_j^{n-1}} + \frac{q_j^n}{P_j^n}\right), \tag{34}$$

with $I_j^0 = 0$. Then the second-order approximation of the TBC operator (22) can be written as

$$\Lambda_2^n = \Lambda_1^n + \mathrm{i}\frac{dV_j^n}{4}P_j^n I_j^n, \tag{35}$$

where

$$dV_j^n = \frac{2}{\Delta x}(q_{j+1}^n\overline{q_{J-j}^n} - 2q_j^n\overline{q_{J-j}^n} + q_j^n\overline{q_{J-j-1}^n}).$$

Again, one can calculate the values of the wave function at the boundaries by solving the system of nonlinear equations with respect to q_j^n, given by

$$\frac{q_1^n - q_0^n}{\Delta x} - e^{-\mathrm{i}\pi/4}\sqrt{\frac{2}{\Delta t}}P_0^n \sum_{k=0}^{n}\left(\beta_k \frac{q_0^{n-k}}{P_0^{n-k}}\right) - \mathrm{i}\frac{dV_0^n}{4}P_0^n I_0^n, \tag{36a}$$

$$\frac{q_J^n - q_{J-1}^n}{\Delta x} + e^{-\mathrm{i}\pi/4}\sqrt{\frac{2}{\Delta t}}P_J^n \sum_{k=0}^{n}\left(\beta_k \frac{q_J^{n-k}}{P_J^{n-k}}\right) + \mathrm{i}\frac{dV_J^n}{4}P_J^n I_J^n. \tag{36b}$$

5. Numerical experiment

In this numerical experiment we solve the nonlocal nonlinear Schrödinger equation given by Eq. (1) on the finite interval $[-L, L]$. On the left ($x = -L$) and right ($x = L$) boundaries we impose the first-order approximation of the TBC (21). For the initial condition, we choose the sum of two analytic solutions (3) that are symmetric about the origin of the spatial coordinate ($x = 0$)

$$q(x, 0) = \frac{\alpha_1}{2}\sqrt{\frac{3\mathrm{i}}{\alpha_1\beta_1}}\Big(G_+(x) + G_-(x)\Big), \tag{37}$$

where

$$G_\pm(x) = \frac{e^{\mp 5\mathrm{i}(x\pm L/2)}}{g_r^\pm + \mathrm{i}g_i^\pm},$$

$$g_r^\pm(x) = \cosh\Big(\frac{-3(x \pm L/2) - \Delta_R}{2}\Big)\cos\Big(\frac{\Delta_I}{2}\Big),$$

$$g_i^\pm(x) = \sinh\Big(\frac{-3(x \pm L/2) - \Delta_R}{2}\Big)\sin\Big(\frac{\Delta_I}{2}\Big)$$

with parameters $\alpha_1 = 1.13 + 1.13\mathrm{i}$, $\beta_1 = 1.13 - 1.13\mathrm{i}$, $\Delta_R = \log\big(\frac{|\alpha_1|^2|\beta_1|^2}{9}\big)$ and $\Delta_I = -\frac{\mathrm{i}}{2}\log\big(\frac{\alpha_1\beta_1}{\alpha_1^*\beta_1^*}\big)$. This choice of double solitons is made to avoid a vanishing of the norm and energy quantities given by Eq. (4).

We chose $L = 6$, and the discretization parameters are chosen as $\Delta x = 0.014$ and $\Delta t = 0.002$. The evolution of the solitons traveling to left and right directions is plotted in Fig. 1, from which it can be seen that the solitons leave the computational domain almost without any reflection.

To analytically quantify the absence of reflection at the boundary of the interval, one can use physically observable quantities in the interval $[-L, L]$. This could be, for example, the ratio of the energy or norm in the interval $[-L, L]$ to those in the whole space. Such ratios in the interval $[-L, L]$ should become zero after time has elapsed. Here we calculate the time dependence of the energy. As can be seen from the plot in Fig. 2, the energy becomes zero after a certain time has elapsed. This means that the ratio of the energy in the interval $[-L, L]$ also becomes zero. Following our simulation, we plot the time dependence of the energy of the solitons restricted to the computational domain. For this purpose, we discretize the energy in Eq. (4) by

$$E_n = \frac{1}{2\Delta x}\sum_{j=1}^{J-1}\Big[(q_{j+1}^n - q_{j-1}^n)(\overline{q_{J-j-1}^n} - \overline{q_{J-j+1}^n}) + 2\Delta x(q_j^n\overline{q_{J-j}^n})^2\Big]. \tag{38}$$

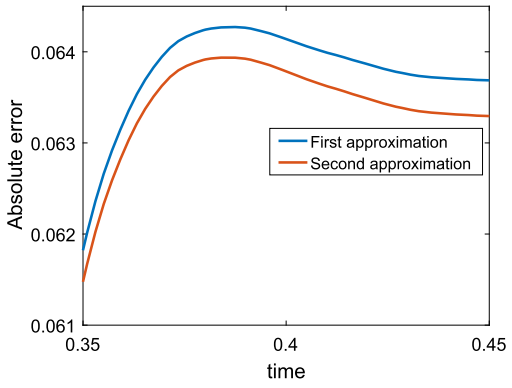

Fig. 3. The plot of the absolute error $||\mathcal{E}||_2^2$ versus time. The considered time interval is the period of interest, when solitons encounter boundaries.

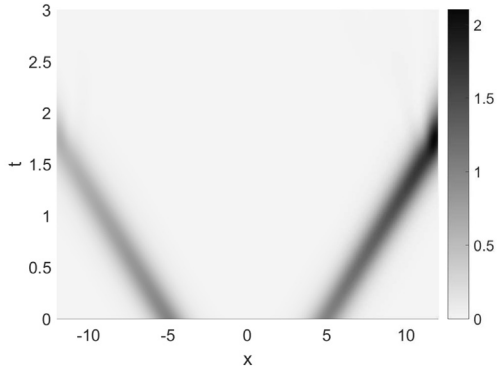

Fig. 4. Evolution of the asymmetric soliton profile given by Eq. (40) with TBCs imposed at both (left and right) end points.

The time dependence of the energy in the computational domain is shown in Fig. 2. This plot shows that the energy vanishes, which means that there are almost no (reflected) waves as time passes.

Finally, we show that the inclusion of the second-order approximation term in the TBC can slightly improve the results. To this end, we calculate the absolute error $\mathcal{E}$, i.e., the difference between the numerical solution with TBC imposed at $x = \pm L$ and the numerical solution for the extended interval $[-2L, 2L]$ (such that boundaries are not reached within the considered time frame) restricted to $[-L, L]$, measured with the L^2-norm (discretized by the trapezoidal rule)

$$||\mathcal{E}||_2^2 = \Delta x \left[\sum_{j=1}^{J-1} \Delta q_j^n \Delta \overline{q_{J-j}^n} + \frac{1}{2} (\Delta q_0^n \Delta \overline{q_J^n} + \Delta q_J^n \Delta \overline{q_0^n}) \right], \qquad (39)$$

where $\Delta q_j^n = q_j^n - Q_j^n$ and Q_j^n is the numerical solution for the extended interval. This is done to exclude the discretization error caused by the finite-difference scheme and to compare only errors caused by the approximations of TBCs. The plot of this error versus time for the time period of solitons' leaving is shown in Fig. 3.

Here we also consider the asymmetric case, i.e. the case of asymmetric solitons. To do this, we use variational solutions in the numerical solution of the NNLS equation with TBC as initial conditions, which are described in Ref. [25]:

$$\begin{aligned} q(x,0) &= \sum_{j=1}^{2} q_j(x,0), \\ q_j(x,0) &= A_j \exp(\mathrm{i}B_j)\ \mathrm{sech}[C_j(x - X_j)] \\ &\times \exp\left[\mathrm{i}D_j(x - X_j)^2 + \mathrm{i}E_j(x - X_j)\right], \end{aligned} \qquad (40)$$

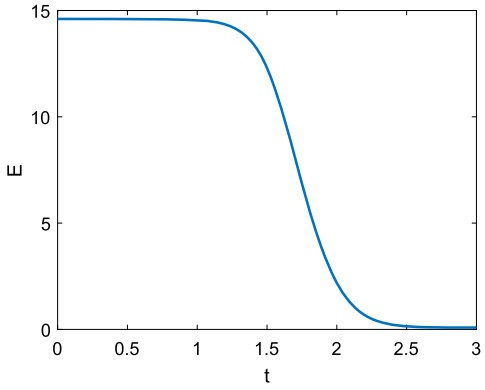

Fig. 5. Energy vs. time in the finite domain $x \in [-L, L]$ for the case of an asymmetric soliton evolution.

where $A_1 = A_2 = 1$, $B_1 = 0$, $B_2 = 0.1$, $C_1 = C_2 = 1$, $D_1 = D_2 = 0$, $E_1 = -E_2 = 2$, $X_1 = -X_2 = 5$. The evolution of the traveling asymmetric soliton is shown in Fig. 4. It shows similar dynamics as the symmetric counterpart, i.e. no reflection is visible. As an additional confirmation of the reflectionless propagation of the asymmetric soliton, we have plotted in Fig. 5 the time dependence of the energy confined to the finite interval $[-L, L]$. The plot shows that TBC also works in these cases.

6. Conclusions

In this work, we have derived transparent boundary conditions (TBCs) for the nonlocal nonlinear Schrödinger equation using the so-called potential approach. Such boundary conditions allow to obtain the solution of an initial value problem given in an interval, which is equal to the solution of the problem for the whole space confined in this interval. The discretization of the derived TBCs and their numerical implementation were presented in detail.

The confirmation of the nearly reflectionless transition by artificial boundaries was achieved by the simulation of traveling solitons. The time dependence of the energy in the computational domain was calculated to verify the obtained results. Although the first-order approximation of the TBC shows good results, the additional second-order terms are also considered to show that the absolute error decreases in this case (which is natural). Although TBCs are commonly used for numerical simulations, they can also be explained from a physical point of view: The incoming wave does not "feel" the boundary where the TBC is imposed, which ensures that there is no or minimal loss in the transmission of waves from one domain to another.

The above model can be used for the development and design of PT-symmetric optical waveguides that allow quasi-reflectionless propagation of solitons. The practical application of such functional materials in optoelectronic devices would allow to save resources and improve performance by reducing signal losses. Finally, we note that the above consideration can be directly extended to optical waveguide networks by determining physically relevant conditions for the transparency of the branching points of the network. Such structures are even more attractive from the point of view of optoelectronic applications. A corresponding study is currently in progress.

CRediT authorship contribution statement

M.E. Akramov: Visualization, Investigation. **J.R. Yusupov:** Writing – original draft, Validation, Methodology. **M. Ehrhardt:** Writing – review & editing, Supervision, Conceptualization. **H. Susanto:** Writing – review & editing, Validation. **D.U. Matrasulov:** Writing –

review & editing, Writing – original draft, Supervision, Project administration.

Declaration of competing interest

The authors declare that they have no known competing financial interests or personal relationships that could have appeared to influence the work reported in this paper.

Data availability

No data was used for the research described in the article.

Acknowledgement

The work is supported by the grant of the Ministry for Innovation Development of Uzbekistan (Ref. No. F-2021-440). One of the authors (DM) thanks the Associates Program of the Abdus Salam ICTP for his hospitality during his visit. H.S. also acknowledges support from Khalifa University through a Faculty Start-Up Grant (No. 8474000351/FSU-2021-011).

References

[1] M. Ehrhardt, Appl. Numer. Math. 58 (5) (2008) 660.
[2] X. Antoine, Ch. Besse, S. Descombes, SIAM J. Numer. Anal. 43 (2006) 2272.
[3] Z. Xu, H. Han, Phys. Rev. E 74 (2006) 037704.
[4] A. Zisowsky, M. Ehrhardt, Math. Comput. Model. 47 (2008) 1264.
[5] J. Zhang, Z. Xu, X. Wu, Phys. Rev. E 79 (2009) 046711.
[6] R. Hammer, W. Pötz, A. Arnold, J. Comput. Phys. 256 (2014) 728.
[7] M.J. Gander, L. Halpern, Math. Comput. 74 (2004) 153.
[8] X. Antoine, E. Lorin, Q. Tang, Mol. Phys. 115 (2017) 1861.
[9] C. Zheng, SIAM J. Sci. Comput. 29 (6) (2007) 2494.
[10] H. Han, Z. Zhang, Appl. Numer. Math. 59 (2009) 1568.
[11] H. Li, X. Wu, J. Zhang, Phys. Rev. E 84 (2011) 036707.
[12] M.M. Aripov, K.K. Sabirov, J.R. Yusupov, Nanosyst., Phys. Chem. Math. 10 (5) (2019) 501–602.
[13] J.R. Yusupov, K.K. Sabirov, Q.U. Asadov, M. Ehrhardt, D.U. Matrasulov, Phys. Rev. E 101 (6) (2020) 062208.
[14] M.J. Ablowitz, Z.H. Musslimani, Phys. Rev. Lett. 110 (2013) 064105.
[15] S. Stalin, M. Senthilvelan, M. Lakshmanan, Phys. Lett. A 377 (2017) 860.
[16] M.J. Ablowitz, Z.H. Musslimani, Phys. Rev. E 90 (2014) 032912.
[17] M.J. Ablowitz, Z.H. Musslimani, Nonlinearity 29 (2016) 915.
[18] M.J. Ablowitz, Z.H. Musslimani, Stud. Appl. Math. 139 (2016) 7.
[19] D. Sinha, P.K. Ghosh, Phys. Rev. E 91 (2018) 042908.
[20] J. Yang, Phys. Rev. E 98 (2018) 042202.
[21] Z. Wen, Zh. Yan, Chaos 27 (2017) 053105.
[22] B-F. Feng, X-D. Luo, M.J. Ablowitz, Z.H. Musslimani, Nonlinearity 31 (2018) 5385.
[23] M.J. Ablowitz, X-D. Luo, Z.H. Musslimani, J. Math. Phys. 59 (2018) 011501.
[24] M.J. Ablowitz, Z.H. Musslimani, J. Phys. A 52 (2019) 15LT02.
[25] R. Rusin, R. Kusdiantara, H. Susanto, Phys. Lett. A 383 (2019) 2039.
[26] J. Rao, J. He, T. Kanna, D. Mihalache, Phys. Rev. E 102 (2020) 032201.
[27] C.B. Ward, P.G. Kevrekidis, T.P. Horikis, D.J. Frantzeskakis, Phys. Rev. Res. 2 (2020) 013351.
[28] M. Akramov, K. Sabirov, D. Matrasulov, H. Susanto, S. Usanov, O. Karpova, Phys. Rev. E 105 (2022) 054205.
[29] O. Maor, N. Dror, B.A. Malomed, Opt. Lett. 38 (2013) 5454–5457.
[30] K.K. Sabirov, J.R. Yusupov, M.M. Aripov, M. Ehrhardt, D.U. Matrasulov, Phys. Rev. E 103 (2021) 043305.
[31] A. Durán, J.M. Sanz-Serna, IMA J. Numer. Anal. 20 (2000) 235.